Drifting Arctic sea ice archives changes in ocean surface conditions

Stephanie Pfirman
Environmental Science Department, Barnard College, Columbia University, New York, New York, USA

William Haxby
Lamont-Doherty Earth Observatory, Columbia University, Palisades, New York, USA

Hajo Eicken and Martin Jeffries
Geophysical Institute, University of Alaska Fairbanks, Fairbanks, Alaska, USA

Dorothea Bauch
Leibniz-Institut für Meereswissenschaften an der Universität Kiel (IFM-GEOMAR), Kiel, Germany

Received 3 June 2004; accepted 3 September 2004; published 8 October 2004.

[1] $\delta^{18}O$ profiles in drifting Arctic sea ice are coupled with back trajectories of ice drift and an ice growth model to reconstruct the surface hydrography of the Arctic Ocean interior. The results compare well with $\delta^{18}O$ values obtained by traditional oceanographic methods and known water mass distributions. Analysis of the stable isotopic composition of sea ice floes sampled at strategic and relatively accessible locations, e.g., Fram Strait, could aid in mapping spatial and temporal variations in Arctic Ocean surface waters. *INDEX TERMS:* 4207 Oceanography: General: Arctic and Antarctic oceanography; 1863 Hydrology: Snow and ice (1827); 4283 Oceanography: General: Water masses 4215 Oceanography: General: Climate and interannual variability (3309); 1860 Hydrology: Runoff and streamflow. **Citation:** Pfirman, S., W. Haxby, H. Eicken, M. Jeffries, and D. Bauch (2004), Drifting Arctic sea ice archives changes in ocean surface conditions, *Geophys. Res. Lett.*, *31*, L19401, doi:10.1029/2004GL020666.

1. Introduction

[2] The perennially ice-covered Arctic Ocean is difficult to access for oceanographic investigations. In the past, limited measurements taken in different regions and years by arduous and expensive field investigations, were compiled to map circumpolar distributions of water masses (Figure 1). Comparisons of temperature, salinity, $\delta^{18}O$ and other tracers along oceanic transects indicate that during the past two decades the distribution of Atlantic water and river runoff has varied dramatically [e.g., *Carmack et al.*, 1997; *Morison et al.*, 1998; *Steele and Boyd*, 1998; *Maslowski et al.*, 2000; *Ekwurzel et al.*, 2001; *Björk et al.*, 2002; *Boyd et al.*, 2002; *Schlosser et al.*, 2002]. These changes in the distribution of water masses have profound effects on climate, including the global meridional overturning circulation, and require an assessment of water-mass distribution on shorter space and time scales.

[3] Validating the timing and location of the shifts in surface hydrography in the interior Arctic Ocean is difficult, because sampling requires access from icebreakers, aircraft, or submarines. Here we show that sea ice – the very substance that hinders direct measurements – can be used as an archive of upstream water mass properties. Level sea ice thickens primarily by ice growth on the bottom as it drifts for several years through the Arctic Basin before exiting, generally through Fram Strait or the Barents Sea. Depending on location and responding largely to the winds [*Thorndike and Colony*, 1982], multiyear ice floes can drift ca. 1000 km/yr over surface waters with markedly different characteristics (Figure 1).

[4] Stable oxygen isotopes are especially valuable tracers in investigations of Arctic surface water masses [*Ostlund and Hut*, 1984; *Schlosser et al.*, 1995; *Bauch et al.*, 1995; *Ekwurzel et al.*, 2001; *Macdonald et al.*, 2002]. $\delta^{18}O$, the ratio of ^{18}O to ^{16}O in a sample normalized to the ratio in standard seawater (SMOW), is expressed in parts per thousand (‰). Arctic river runoff, derived from precipitation, is depleted in ^{18}O with an average value of -18‰, while Atlantic water is about 0.3‰ and the Pacific Inflow has values around -1‰ [*Ekwurzel et al.*, 2001] (Figure 1).

2. Approach

[5] Our goal is to reconstruct the ocean surface $\delta^{18}O$ field in inaccessible regions, using $\delta^{18}O$ profiles from sea ice cores coupled with back trajectories of ice drift and a simple ice growth model. This approach requires that the floes thicken by bottom ice growth without significant deformation, downcore sampling frequency must be adequate to minimize effects of volume averaging, the back trajectories must be accurate, $\delta^{18}O$ must be conservative, fractionation factors must be known, and basal ice accretion and melting must be estimated through an ice growth model. Profiles of $\delta^{18}O$ are from sea ice cores obtained in 1989 (3 cores Barents Sea), 1991 (12 cores Eurasian Basin), 1992 (31 cores Chukchi Sea), 1993 (19 cores Beaufort Sea), 1994 (7 cores Transpolar Drift), and 1995 (24 cores Laptev Sea). Cores were collected from level ice that, based on stratigraphic analysis, was mostly undeformed and had thickened by bottom growth, with rafted ice excluded from the analysis. Cores were sampled at ca. 10 cm intervals, which appears to provide sufficient resolution (see profiles in Figure 2: a 2.5 m core would produce 25 samples over 3 years or ca. 3000 km, resulting in a sample on average every 90 km during the ca. 9 month ice growth season).

0094-8276/04/2004GL020666$05.00

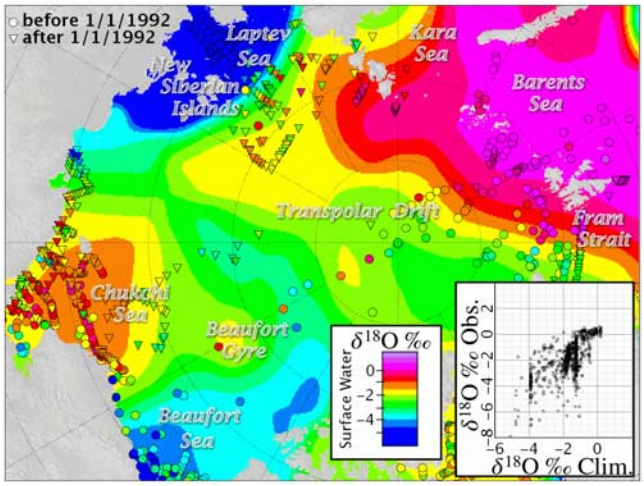

Figure 1. Surface $\delta^{18}O$ climatology (gridded field compiled from $\leq$25 m samples, derived by weighted averages) and $\leq$25 m surface water samples from G. A. Schmidt et al. (Global seawater oxygen-18 database, 1999, available at http://www.giss.nasa.gov/data/o18data/) (circles: sampled before 1/1/1992, triangles: sampled after 1/1/1992). Scatter plot shows water samples vs. climatology.

Back trajectories of ice drift were calculated based on a combination of remote sensing and buoys from the International Arctic Buoy Program (IABP [*Fowler*, 2003]), with an estimated error of ca. 100 km/year [e.g., *Pfirman et al.*, 1997]. Theoretical work [*Eicken*, 1998] and analysis of decades to centuries old sea ice samples [*Jeffries*, 1991] indicates that $\delta^{18}O$ is conservative: ice desalination through brine drainage does not significantly affect the bulk isotopic composition. Downward flushing of snow meltwater alters the composition of the uppermost 0.2 to 0.4 m (see top part of core profiles in Figure 2) but is of lesser importance below the freeboard layer [*Eicken et al.*, 2002]. Therefore, the top 10% of each core was excluded from this analysis. Outliers, deviating >2‰ from adjacent values, were also excluded.

[6] During sea ice formation, ^{18}O is preferentially incorporated into ice over ^{16}O compared with the parent water. Fractionation varies from <0.1‰ for fast growing (>10 mm h^{-1}) frazil ice up to >2.5‰ for slow growing (<0.01 mm h^{-1}) columnar ice [*Eicken*, 1998]. Most of the ice used in this analysis was columnar multiyear ice and grew slowly at the base of a 1–3 m thick ice column. For typical multiyear floes of 2 m thickness, basal ice growth rates would vary between 0.1 and 2.0 cm d^{-1} during winter, resulting in theoretical fractionation of 1.6 to 2.5‰ [*Eicken*, 1998]. Field measurements [e.g., *Melling and Moore*, 1995; *Macdonald et al.*, 2002], and results from this analysis (e.g. scatter plots and profiles in Figure 2) indicate that 2‰ is a reasonable fractionation value for drifting multiyear ice.

[7] In addition to snow melt influencing the ice surface, both under-ice melt ponds and some summer ice layers have depleted $\delta^{18}O$ values characteristic of admixtures of snow melt (Figure 2a) [*Jeffries et al.*, 1989, 1995; *Eicken et al.*, 2002]. Such annual layers are sometimes accompanied by biogenic inclusions and/or changes in ice crystallography. Annual layers are of assistance, because they provide a time stamp indicative of summertime ice accretion, and aid in validation of the ice growth model (Figure 2). Clearly identified underice meltponds were removed prior to back trajectory mapping because they do not represent the regional isotopic composition of the surface ocean.

3. Ice Growth Model

[8] In order to relate ice core depths to dates on the back trajectories, we employed a simple ice growth model. Ice

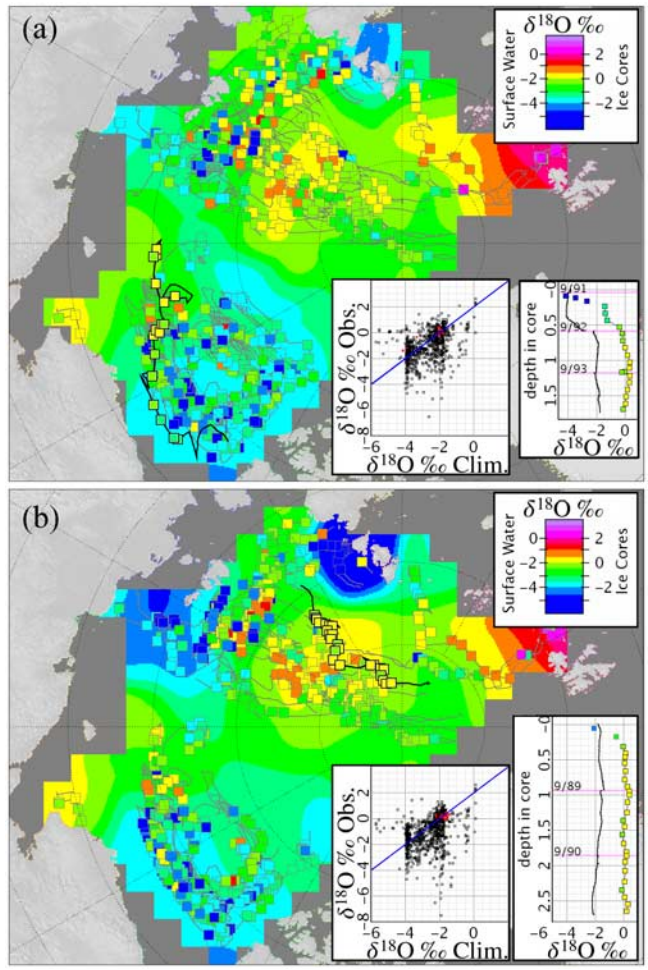

Figure 2. (a) Gridded reconstructed ocean surface $\delta^{18}O$ for 1986–1995 derived from sea ice samples (squares) laid down upon back trajectories (lines) with k_{snow} = 0.2 W m^{-1} K^{-1}. Ocean color scale shifted by 2‰ to account for fractionation during ice formation. Core profile compares ice core $\delta^{18}O$ with a reconstructed profile based on the ice growth model and back mapping the floe trajectory though the climatological surface ocean $\delta^{18}O$ field (Figure 1). Annual layer at 120 cm has depleted $\delta^{18}O$ signature reflecting refrozen snow melt. Timing fits modeled result of layer formation during summer 1993. Note offset between the measured and reconstructed $\delta^{18}O$ profile confirming ca. +2‰ fractionation during ice formation, and the 2‰ offset in the scatter plot of climatology vs. ice samples. (b) As in Figure 2a but using k_{snow} = 0.5 W m^{-1} K^{-1}. Modeled summer dates match annual layers defined by crystallographic analysis and incorporated biogenic material at 93–95 cm and 180–183 cm.

growth is controlled by freezing/melting at the ice bottom, and melting at the surface during the summer. Growth at the ice bottom is modeled by balancing the latent heat of freezing/melting, the ocean heat flux, and the conductive heat loss [e.g., *Thorndike*, 1992]:

$$0 = L \bullet \Delta H/\Delta t + F + (T_{surface} - T_0) \bullet (k_{ice} \bullet k_{snow})/(k_{ice} \bullet H_{snow} + k_{snow} \bullet H_{ice}) \quad (1)$$

where L is the latent heat of fusion ($3 \bullet 10^8$ J m^{-3}), $\Delta H/\Delta t$ is the ice growth rate, H is layer thickness, F is the ocean heat flux, T is temperature ($T_0 = -1.9$°C at the ice-water interface), and k is thermal conductivity ($k_{ice} = 2$ W m^{-1} K^{-1}, $k_{snow} \approx 0.33$ W m^{-1} K^{-1}). Following the back trajectory for each ice core, the daily ice growth increment was computed from equation (1), using snow depth estimates from *Warren et al.* [1999], estimates of ocean heat flux from modeling by *Zhang et al.* [2000], and daily mean temperatures from the IABP database [*Rigor et al.*, 2000]. The rate of melting at the surface during the summer was set to 0.005 m d^{-1}, consistent with total summer melt used by *Thorndike* [1992].

[9] The ice growth model assigns a date to each sample in each core. The back-trajectories in turn yield a sample's geographic location. If the model underestimates the growth rate (e.g., by overestimating snow depth) then the samples will be assigned dates that are too early, and the assigned locations will be too spread out along the trajectory. Fortunately, we can use annual layers in some cores to adjust the model parameters, specifically the thermal conductivity of snow (k_{snow}), to match observed and simulated growth history. Higher k_{snow} means faster growth, which also could be caused by thinner snow, lower air temperature, or lower ocean heat flux. A lower summer melt rate also results in faster growth rates (because we model the growth in reverse), but is relatively more important for thick, slow-growing ice. For the 11 cores where annual layers could be accurately matched, k_{snow} varied between 0.2 and 0.5 W m^{-1} K^{-1} (Figure 2) with a median and average of 0.3 W m^{-1} K^{-1}.

4. Regional Variations

[10] The ocean surface δ^{18}O values from ice cores (Figure 2) reconstruct the main features observed in the climatology derived from ocean water samples (Figure 1). Ice cores from the Transpolar Drift consistently indicate ^{18}O-depleted surface waters near the North Pole and higher values representing Atlantic influence in the Barents Sea boundary region. Elevated values north of the New Siberian Islands also manifest the influence of Atlantic water passing to the northeast of this archipelago. On the other side of the Arctic, the Pacific inflow shows up clearly in cores from ice that drifted through the Chukchi Sea. As expected, ice accreted in the Beaufort Gyre with its reservoir of river water retains a depleted isotopic signature. Data archived by drifting sea ice fills in regions poorly resolved by direct sampling from ships: northeast of the New Siberian Islands, the central Beaufort Gyre, and the central axis of the Transpolar Drift.

5. Variability

[11] What causes the variability in reconstructed values and the deviations from the climatology? In this analysis we eliminated obvious refrozen underice meltponds, but we retained the summer ice layers, corresponding to samples with anomalously low δ^{18}O (dark blue points in Figure 2). Some of the variability is likely due to errant trajectories, undetected layers of ice rafted from different source regions, and sampling or analytical errors. The weighted averaged contouring in regions of sparse data possibly introduces artifacts including the segregation into two pools of Atlantic-origin waters, and the extension of Atlantic and river influence into the central basin with little or no data. The degree of variability of the multiyear central Arctic (1991 and 1994) samples is significantly smaller than those collected over the Barents, Chukchi, Beaufort and Laptev Sea shelves. A detailed analysis of 1995 Laptev Sea ice cores established that spatio-temporal variations are due to steep gradients in surface water composition and complex shelf circulation patterns, including the recirculation of first- and second-year ice [*Eicken et al.*, 2000].

[12] On a pan-Arctic scale, the reconstructed δ^{18}O field is more negative than the climatology: although 2‰ fractionation fits the offset in individual multiyear cores and the bulk of the data (Figure 2), the average offset between the ocean climatology and the reconstructions is 1.45‰ for $k_{snow} = 0.5$ W m^{-1} K^{-1} and 1.65‰ for $k_{snow} = 0.2$ W m^{-1} K^{-1}. The Pacific Inflow appears less influential in the ice core reconstruction (Figure 2), based on 1992 and 1994 samples, than in the climatology, based on a mix of pre- and post-1992 data (Figure 1). A weakened Pacific inflow is supported by tracer analysis [*Ekwurzel et al.*, 2001], documenting a decrease in the influence of the Pacific Water mass in the central Arctic between 1991 and 1994. Increasing river run-off from Siberian rivers [*Ye et al.*, 2003] would also result in reduced δ^{18}O values.

[13] Siberian river influence is more extensive in the reconstruction north and east of the Kara Sea near Severnaya Zemlya and north of the East Siberian Sea, compared to climatology. The latter is not well constrained off Severnaya Zemlya (Figure 1), but increased Ob and Yenisey river influence in this region is possible. During 1993 and 1994, other investigators noted extensive flow of river runoff along the shelf to the east, with some offshelf flow occurring north of the New Siberian Islands (ca. 140°E) but most leaving the shelf at the Mendeleyev Ridge (ca. 170°E [*Steele and Boyd*, 1998; *Maslowski et al.*, 2000; *Ekwurzel et al.*, 2001; *Guay et al.*, 2001; *Boyd et al.*, 2002]). The region of proposed offshelf flow is in the vicinity of the depleted values mapped by the reconstruction. Some Laptev Sea ice cores reflect winter ice growth following the summer of 1994 when river runoff was apparently confined to the inner shelf [*Eicken et al.*, 2000; *Guay et al.*, 2001].

[14] The Beaufort Gyre values, reconstructed largely from ice samples obtained in 1992 and 1993, are more depleted than the climatology, which is based on relatively few samples obtained largely prior to 1992. This change is consistent with increased river influence in this region in 1992 compared with the years before and after [*Macdonald et al.*, 1999]. *Maslowski et al.* [2000] also modeled a substantial increase in river water transport to the Beaufort Gyre during the period 1979 to 1993.

[15] In the Eurasian Arctic, there was less river runoff and extended influence of Atlantic water from 1991 to 1998 [e.g., *Carmack et al.*, 1997; *Steele and Boyd*, 1998; *Boyd et*

al., 2002; *Schlosser et al.*, 2002]. North of the New Siberian Islands, cores obtained primarily in 1989 through 1995 match the elevated $\delta^{18}O$ distribution in the climatology, representing Atlantic influence in this region. However, within and north of the Barents Sea, the Atlantic water signature in the reconstruction is markedly subdued because the reconstruction represents earlier conditions: it is largely based on a few cores obtained in the Barents Sea in 1989 and the Transpolar Drift in 1991. Also, increased heat flux from strongly Atlantic-influenced waters may diminish ice growth or melt the ice underside [*Steele and Boyd*, 1998; *Björk et al.*, 2002] to the extent that Atlantic signatures are underrepresented.

6. Conclusions

[16] $\delta^{18}O$ signatures preserved in drifting Arctic sea ice record and archive the $\delta^{18}O$ signatures of ocean surface waters. The main features of the $\delta^{18}O$ field of the central Arctic can be reconstructed from sea ice cores, allowing for indirect mapping of the surface water mass distribution. This method cannot substitute for direct sampling: limitations include modeling ice accretion and melt, errant trajectories, variable fractionation, discontinuous records due to lack of ice formation or basal melt, and undetected ice rafting. However, annual sampling of sea ice at the North Pole and peripheral ice exit locations (Fram Strait, Barents and Beaufort seas) would provide ice that had drifted over large areas and would be a cost-effective means of estimating spatial and temporal variations in oceanic frontal boundaries in the ice-bound interior of the Arctic Ocean.

[17] **Acknowledgments.** Support: NSF DPP 91-22948, OPP 94-00144, 97-08924, 98-76843, Mellon Fdtn; sampling, analysis, discussion: T. Tucker & T. Gow (CRREL), D. Pederson & R. Mortlock (LDEO).

References

Bauch, D., P. Schlosser, and R. G. Fairbanks (1995), Freshwater balance and the sources of deep and bottom waters in the Arctic Ocean inferred from the distribution of $H_2{}^{18}O$, *Prog. Oceanogr.*, *35*, 53–80.

Björk, G., J. Söderkvist, P. Winsor, A. Nikolopoulos, and M. Steele (2002), Return of the cold halocline layer to the Amundsen Basin of the Arctic Ocean: Implications for the sea ice mass balance, *Geophys. Res. Lett.*, *29*(11), 1513, doi:10.1029/2001GL014157.

Boyd, T. J., M. Steele, R. D. Muench, and J. T. Gunn (2002), Partial recovery of the Arctic Ocean halocline, *Geophys. Res. Lett.*, *29*(14), 1657, doi:10.1029/2001GL014047.

Carmack, E. C., K. Aagaard, J. H. Swift, R. W. MacDonald, F. A. McLaughlin, E. P. Jones, R. G. Perkin, J. N. Smith, K. M. Ellis, and L. R. Killius (1997), Changes in temperature and tracer distributions within the Arctic Ocean: Results from the 1994 Arctic Ocean, *Deep Sea Res.*, *Part II*, *44*, 1487–1502.

Eicken, H. (1998), Factors determining microstructure, salinity and stable-isotope composition of Antarctic sea ice: Deriving modes and rates of ice growth in the Weddell Sea, *Antarctic Sea Ice Physical Processes, Interactions and Variability, Antartc. Res. Ser.*, vol. 74, edited by M. O. Jeffries, pp. 89–122, AGU, Washington, D. C.

Eicken, H., J. Kolatschek, J. Freitag, F. Lindemann, H. Kassens, and I. Dmitrenko (2000), Identifying a major source area and constraints on entrainment for basin-scale sediment transport by Arctic sea ice, *Geophys. Res. Lett.*, *27*, 1919–1922.

Eicken, H., H. R. Krouse, D. Kadko, and D. K. Perovich (2002), Tracer studies of pathways and rates of meltwater transport through Arctic summer sea ice, *J. Geophys. Res.*, *107*(C10), 8046, doi:10.1029/2000JC000583.

Ekwurzel, B., P. Schlosser, R. A. Mortlock, R. G. Fairbanks, and J. H. Swift (2001), River runoff, sea ice meltwater, and Pacific water distribution and mean residence times in the Arctic Ocean, *J. Geophys. Res.*, *106*(C5), 9075–9092.

Fowler, C. (2003), Polar Pathfinder daily 25 km EASE-grid sea ice motion vectors, http://nsidc.org/data/nsidc-0116.html, Natl. Snow and Ice Data Cent., Boulder, Colo.

Guay, C. K. H., K. K. Falkner, R. D. Muench, M. Mensch, M. Frank, and R. Bayer (2001), Wind-driven transport pathways for Eurasian Arctic river discharge, *J. Geophys. Res.*, *106*(C6), 11,469–11,480.

Jeffries, M. O. (1991), Massive, ancient sea ice strata and preserved physical-structural characteristics in the Ward Hunt Ice Shelf, *Ann. Glaciol.*, *15*, 125–131.

Jeffries, M. O., H. R. Krouse, W. M. Sackinger, and H. Serson (1989), Stable isotope ($^{18}O/^{16}O$) tracing of fresh, brackish and sea ice in multiyear landfast sea ice, Ellesmere Island, Canada, *J. Glaciol.*, *35*(119), 9–16.

Jeffries, M. O., K. Schwartz, K. Morris, A. D. Veazey, H. R. Krouse, and S. Cushing (1995), Evidence for platelet ice accretion in Arctic sea ice development, *J. Geophys. Res.*, *100*(C6), 10,905–10,914.

Macdonald, R. W., E. C. Carmack, F. A. McLaughlin, K. K. Falkner, and J. H. Swift (1999), Connections among ice, runoff, and atmospheric forcing in the Beaufort Gyre, *Geophys. Res. Lett.*, *26*, 2223–2226.

Macdonald, R. W., F. A. McLaughlin, and E. C. Carmack (2002), Fresh water and its sources during the SHEBA drift in the Canada Basin of the Arctic Ocean, *Deep Sea Res.*, *Part I*, *49*, 1769–1785.

Maslowski, W., B. Newton, P. Schlosser, A. Semtner, and D. Martinson (2000), Modeling recent climate variability in the Arctic Ocean, *Geophys. Res. Lett.*, *27*, 3743–3746.

Melling, H., and R. M. Moore (1995), Modification of halocline source waters during freezing on the Beaufort Sea shelf; evidence from oxygen isotopes and dissolved nutrients, *Cont. Shelf Res.*, *15*, 89–113.

Morison, J., M. Steele, and R. Anderson (1998), Hydrography of the upper Arctic Ocean measured from the nuclear submarine U.S.S. Pargo, *Deep Sea Res.*, *Part I*, *45*, 15–38.

Ostlund, H. G., and G. Hut (1984), Arctic Ocean water mass balance from isotope data, *J. Geophys. Res.*, *89*(C4), 6373–6381.

Pfirman, S. L., R. Colony, D. Nürnberg, H. Eicken, and I. Rigor (1997), Reconstructing the origin and trajectory of drifting Arctic sea ice, *J. Geophys. Res.*, *102*(C6), 12,575–12,586.

Rigor, I., R. Colony, and S. Martin (2000), Variations in surface air temperature observations in the Arctic, 1979–1997, *J. Clim.*, *13*, 896–914.

Schlosser, P., D. Bauch, R. Fairbanks, and G. Bonisch (1995), Arctic river-runoff–mean residence time on the shelves and in the halocline, *Deep Sea Res.*, *Part I*, *41*, 1053–1068.

Schlosser, P., R. Newton, B. Ekwurzel, S. Khatiwala, R. Mortlock, and R. Fairbanks (2002), Decrease of river runoff in the upper waters of the Eurasian Basin, Arctic Ocean, between 1991 and 1996: Evidence from $\delta^{18}O$ data, *Geophys. Res. Lett.*, *29*(9), 1289, doi:10.1029/2001GL013135.

Steele, M., and T. Boyd (1998), Retreat of the cold halocline layer in the Arctic Ocean, *J. Geophys. Res.*, *103*(C5), 10,419–10,435.

Thorndike, A. S. (1992), A toy model linking atmosphere thermal radiation and sea ice growth, *J. Geophys. Res.*, *97*(C6), 9401–9410.

Thorndike, A. S., and R. Colony (1982), Sea ice motion in response to geostrophic winds, *J. Geophys. Res.*, *87*(C8), 5845–5852.

Warren, S. G., I. G. Rigor, V. F. Radinov, N. N. Bryazgin, Y. I. Aleksandrov, and R. Colony (1999), Snow depth on Arctic ice, *J. Clim.*, *9*, 1814–1829.

Ye, B., D. Yang, and D. L. Kane (2003), Changes in Lena River streamflow hydrology: Human impacts versus natural variations, *Water Resour. Res.*, *39*(7), 1200, doi:10.1029/2003WR001991.

Zhang, J., D. Rothrock, and M. Steele (2000), Recent changes in Arctic sea ice: The interplay between ice dynamics and thermodynamics, *J. Clim.*, *13*, 3099–3114.

D. Bauch, Leibniz-Institut für Meereswissenschaften an der Universität Kiel (IFM-GEOMAR), Kiel, Germany.

H. Eicken and M. Jeffries, Geophysical Institute, University of Alaska Fairbanks, Fairbanks, AK, USA.

W. Haxby, Lamont-Doherty Earth Observatory, Columbia University, Palisades, NY, USA.

S. Pfirman, Environmental Science Department, Barnard College, Columbia University, 3009 Broadway, New York, NY 10027, USA. (spfirman@barnard.columbia.edu)